Theor Chim Acta (1994) 88: 201–216

Theoretica Chimica Acta

Long-range interactions in H–He: *ab initio* potential, hyperfine pressure shift and collision-induced absorption in the infrared*

Wilfried Meyer[1] and Lothar Frommhold[2]

[1] Fachbereich Chemie der Universität Kaiserslautern, D-6750 Kaiserslautern, Germany
[2] Physics Department, University of Texas at Austin, Austin, TX 78712-1081, USA

Received April 27, 1993/Accepted July 20, 1993

Summary. The collisional complex H–He, with both atoms in their electronic ground-states, is treated as a molecule in self-consistent field (SCF) and multi-reference configuration interaction (MR-CI) calculations to determine interaction energy, dipole moment and spin density as function of internuclear separation. A basis set tailored for long-range interactions was used and the basis set superposition errors were controlled. The resulting functions are analyzed and presented in analytical form, in terms of exchange and damped dispersion contributions. For all three properties there is full agreement with the accurately known long-range coefficients, but the dipole moment function shows rather large overlap effects even at large distances which obscure higher-order dispersion coefficients. The well depth of 22.56 μE_h is significantly deeper than most recent *ab initio* calculations and model potentials have suggested, but our number corroborates existing semi-empirical values. Likewise, the calculated spin density variations are more pronounced than recent work has suggested. The resulting hyperfine pressure shift of H atoms in a helium buffer gas is in very good agreement with experiment, except for temperatures of the order of 1 K. Infrared absorption continua associated with the induced dipole moment are evaluated for their astrophysical interest.

Key words: H–He – SCF – MR–CI – Interaction energy – Dipole moment – Spin density

1 Introduction

The H–He pair may be considered the simplest van der Waals complex next to $H_2(^3\Sigma_u)$. It probably has the smallest well depth of any atom–atom pair. As a heteronuclear open-shell system, the H–He pair offers a unique opportunity to study the various interaction-induced properties, like dipole moment and hyperfine frequency shifts, in terms of the familiar interaction forces, i.e. exchange repulsion and dispersion attraction. Due to the extremely weak van der Waals forces, this is

* Dedicated to Prof. W. Kutzelnigg on the occasion of his 60th birthday

not a trivial task for either experiment or theory, certainly not for the study of properties which depend on the delicate balance between the attractive and repulsive mechanisms, especially at separations comparable to the potential minimum and the lower repulsive branch. In this region significant discrepancies do indeed exist between the known theoretical efforts to compute potential, hyperfine pressure shifts and induced dipole moment of H–He pairs. Discrepancies also exist between theory and the few experimental data available. Some of these discrepancies have been discussed recently by Tang and Yang [1] in their attempt to model the interaction potential and the interaction-induced hyperfine frequency shifts of H–He pairs. It appears that a theoretical investigation is still missing that matches the accuracy and detail achieved long ago for closed-shell systems like He_2 or $He–H_2$ [2]. It is the purpose of this paper to establish, from extended multireference CI calculations, reliable data for three important properties of the collisional complex H–He.

Potential. For the well region, the most reliable empirical potential of H–He has been obtained by Jochemsen et al. [3]. It is based on the low-temperature diffusion coefficients measured by Hardy et al. [4]. The well of this empirical model is about 20% deeper than the latest, most ambitious *ab initio* calculation, a full configuration interaction (CI) treatment with a relatively large basis set by Knowles et al. [5]. These authors felt confident to reject the empirical value of the well depth [3] on the basis of their computational results, along with a similarly deep well suggested by Scoles' so-called HFD-B model potential [6]. Interestingly, Knowles et al.'s shallower well depth appears to be supported by Tang and Yang's recent model potential [1], which was constructed according to a scheme that was successful for $He–H_2$ and various rare-gas pairs [7].

However, a close inspection of the basis used in Ref. [5] reveals that it is ill designed for representing dispersion forces. It properly accounts only for the leading long-range ($-C_6/R^6$) term and therefore one must actually expect a well that is significantly deeper than their computation suggests. An *ab initio* potential in close agreement with the empirical potential [3] has indeed been obtained earlier by Das, Wagner and Wahl [8], but this support of the empirical, deeper well could be fortuitous because basis set superposition errors were not considered. A clarification from theory is most desirable because the analysis of the experimental data also has uncertainties: The diffusion cross sections are measured with an accuracy of 5%, which leaves an uncertainty of about 10% for the potential [3]; the convergence in the second-order Chapman–Enskog treatment of the diffusion cross section is not established [4]; and there is a crucial dependence of these cross sections on the accurate determination of the temperature of the measurements.

Hyperfine pressure shift. Shifts of the hyperfine frequency of the H atom have been observed, which vary more or less linearly with the buffer gas (here: helium) density. The shift is negative at low temperatures and positive at high temperatures. The hyperfine frequency is dominated by the Fermi contact term and is therefore proportional to the spin density at the site of the proton. The effective density changes during an H–He encounter and the observed shifts are the statistical average of the frequency shift as function of the H–He separation, $a(R)$.

The two latest *ab initio* calculations of the relative shift $\Delta a(R)/a_\infty$ differ by more than a factor of two [9, 10]. The recent model function by Tang and Yang [1] has therefore been recommended as a better model of the hyperfine pressure shift. Their function [1] indeed accounts for the shifts observed at temperatures around 50°C [11, 12] and from -135 to 350°C [13]. However, a distinctive disagreement with

the measurements at 0.5 and 1.2 K [4, 14] points again to problems of that function in the well region of the potential.

Induced dipole. Interatomic repulsion is associated with a small depletion of the electronic charge density in the space between the atoms; attraction augments that charge density slightly. If dissimilar atoms interact, a dipole moment thus arises whose polarity changes sign as the separation R is increased beyond sufficiently large values. In a mixture of dissimilar monatomic gases, this interaction-induced dipole moment causes absorption in the far infrared and gives rise, for example, to the second virial dielectric coefficient. Induced dipole moments of diatoms have been computed from theory in the past, but theoretical results have differed widely in the well region. This situation has been discussed in a review article [15] where we have presented preliminary results similar to those reported here. So far, there are no measurements relating to the induced dipole of H–He pairs, but it has been pointed out [16] that absorption of infrared radiation by H–He pairs is likely to be an important source of opacity of the cooler stellar atmospheres, e.g. those of late stars, where neutral atomic hydrogen and helium exist in sufficient densities. Because of this significance for astrophysics, reliable predictions of infrared absorption of H–He pairs are desirable. The computational procedures used here have been seen in other cases to provide dependable theoretical data [15, 17].

2 Interaction potential

For a molecular system like H–He with only three electrons it would be possible to perform full CI calculations with reasonably large basis sets. But this is unnecessarily expensive and ultimately the size of the basis set would be limited. For H–He at not too small separations, large correlation exists only between the two He electrons. Thus sufficiently converged results can be obtained from a multi-reference (MR)-CI approach, starting from a multi-configuration self-consistent field (MCSCF) wavefunction including the leading intra-He configurations, i.e. $1s^2$, $2s^2$ and $2p^2$. Indeed, using the basis of Ref. [5], we were able to reproduce the results of that full CI treatment [5] with only insignificant differences in the well region[1]. In our calculations we use the multi-reference self-consistent electron pair technique, designed for internally contracted CI [18] employing particularly strong thresholds for convergence.

It is well known that for calculations of van der Waals potentials the choice of a balanced basis set is crucial. Starting from a standard s-function set [19], we have first roughly optimized a 3p, 2d, 1f set for intra-He correlation. This set was then augmented by 2p, 2d, 2f, 1g diffuse functions accounting for higher-order polarizabilities and related dispersion forces up to $-C_{12}/R^{12}$. For H, a set of 3p, 2d, 1f, 1g diffuse functions was chosen to maximize the dispersion attraction at separations R of about 6 bohr. This basis is documented in Table 1. The total nonrelativistic energy of the separated atoms was only 0.001 hartree above the limit and accounts for 98% of the He correlation. The interaction potential obtained from the MR-CI treatment with the basis specified above is given in Table 2

[1] We note, however, that at the separation of $R = 5.0$ bohr agreement was observed only after correcting the potential from the reported 22.56 [5] to 26.56, in units of 10^{-5} E_h, an error obviously caused by a mistake in the superposition correction.

Table 1. Exponents of the GTO basis set. The *s* exponents are from S. Huzinaga [19]. The other exponents are roughly optimized for intra-atom correlation and dispersion. Brackets indicate a contraction. The exponents of H *p*, *d* in brackets [· · ·] are used only for the computation of the dipole moment at $R > 7.5$ bohr

He	s	(3293.694, 488.8941, 108.7723, 30.1799, 9.789653) 3.52261, 1.35436, 0.5561, 0.24092, 0.107951
	p	5.50, 1.50, 0.50, 0.19, 0.070
	d	3.0, 1.0, 0.38, 0.15
	f	2.4, 0.60, 0.20
	g	0.35
H	s	(1170.498, 173.5822, 38.65163, 10.60720, 3.379649) 1.202518, 0.463925, 0.190537, 0.0812406, 0.0285649
	p	0.6, 0.20, 0.08 [0.032]
	d	0.36, 0.12, [0.04]
	f	0.25
	g	0.30

Table 2. Interaction potential of H–He pairs, in 10^{-6} E_h (column marked "total"). The magnitude of the basis set superposition error (bsse) is also given, along with the deviations of the analytical fit (D-fit)

R	SCF	Intra	Inter	Total	Bsse	D-fit
2.00	70043.76	3064.51	− 10307.18	62801.09	− 18.88	− 40.38
2.25	48559.99	2352.66	− 7947.27	42965.38	− 17.16	21.56
2.50	33307.96	1724.89	− 5930.61	29102.24	− 15.23	23.22
2.75	22615.55	1235.30	− 4360.44	19490.41	− 13.10	9.77
3.00	15211.67	873.52	− 3190.41	12894.78	− 11.02	− 1.45
3.50	6709.63	426.87	− 1712.95	5423.55	− 7.81	− 7.21
4.00	2873.81	203.29	− 931.22	2145.88	− 5.74	− 3.51
4.50	1201.04	94.31	− 513.06	782.29	− 4.16	− 0.72
5.00	491.84	42.59	− 286.65	247.78	− 2.91	0.13
5.50	198.09	18.77	− 162.94	53.92	− 2.02	0.14
6.00	78.71	8.10	− 94.64	− 7.83	− 1.35	0.01
6.50	30.93	3.43	− 56.38	− 22.02	− 0.86	− 0.07
6.75	19.32	2.20	− 43.96	− 22.44	− 0.68	− 0.07
7.00	12.04	1.43	− 34.55	− 21.08	− 0.55	− 0.08
7.50	4.65	0.59	− 21.81	− 16.57	− 0.39	− 0.06
8.00	1.79	0.23	− 14.19	− 12.17	− 0.29	− 0.03
9.00	0.26	0.03	− 6.53	− 6.24	− 0.18	0.01
10.00	0.04	0.00	− 3.31	− 3.27	− 0.10	0.02
11.00	0.00	0.01	− 1.81	− 1.80	− 0.05	0.01
12.00	0.00	0.00	− 1.05	− 1.05	− 0.02	0.01
13.00	0.00	0.00	− 0.64	− 0.64	− 0.01	0.01
14.00	0.00	0.00	− 0.41	− 0.41	0.00	0.01
15.00	0.00	0.00	− 0.26	− 0.26	0.00	0.00

(column marked "total"). It has been obtained as the difference between the energies for HH and H + He in the same molecular basis, the common counterpoise correction for superposition errors [20]. The superposition errors amount to only $\approx 3\%$ at the potential minimum and are quite negligible for the repulsive

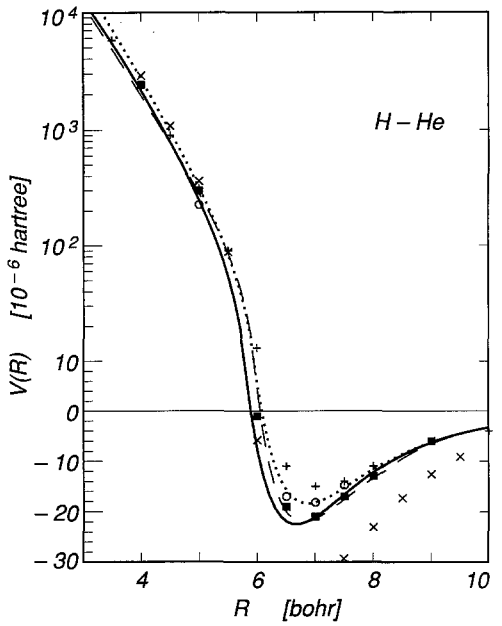

Fig. 1. The interaction potential of H–He: present results (*heavy, solid line*); Scoles' HFD-B model is indistinguishable from the present results in this figure; Jochemsen et al.'s R2 model [3] (*dashes*); Tang and Yang [1] (dots); Das et al. [8] (■); Knowles et al. [5] (○); Davison and Liew [9] (×); Theodorakopoulos et al. [24] (+)

branch of the potential. From the convergence of the dispersion terms, we estimate our potential to be accurate to within 2% or better.

Our potential is compared with some of the most noteworthy previous results in Fig. 1. The curves shown in Fig. 1 are all given by analytical models and use the same low-order dispersion coefficients C_{2n} of Ref. [21]. They are, therefore, in agreement for separations $R > 9$ bohr. Scoles' HFD-B model [6] is not discernible in the figure, since it is virtually identical with the present results (within the width of the heavy line).

Jochemsen et al.'s "R2" semi-empirical potential [3] (dashed) combines the repulsive branch from Gengenbach et al.'s integral cross section measurements [22] with the low-temperature diffusion data of Hardy et al. [4]. This potential is just slightly lower than the present results at small separations ($R < 5$ bohr), rises somewhat above our data for larger R and falls again to slightly smaller values for $R > 7$ bohr. On the whole, the agreement of the R2 model with the present results is remarkably close, certainly as far as well depth, position of the minimum and the repulsive core ($R < 5$ bohr) are concerned. The early computational results of Das, Wagner and Wahl [8] (solid squares) are also rather similar to the present work. The low-energy scattering data of Toennies et al. [23], from which a rather shallow well was deduced, have nevertheless been shown elsewhere [1] to be consistent with the empirical potential [3]. From the close agreement with the latter we infer that our new potential is also consistent with the three sets of experimental data mentioned [4, 22, 23].

Tang and Yang's recent potential model [1] (dotted curve, Fig. 1) is, however, consistently above the present data. Its well depth is a significant 20% smaller. While these results [1] are consistent with Knowles et al.'s CI computations [5], it is clear that their well depth is too small, due to basis set deficiencies, as mentioned above. Another recent calculations yielded an even shallower well [24] (+), but its main emphasis was on excited states. Good agreement is observed at smaller

Table 3. Parameters of the analytical potential model, $V(R)$ of Eqs. (1, 2), representing column 5 of Table 2 with the uncertainties listed, in atomic units; coefficients $C_{12}, \ldots, C_{18}$ according to Eq. (4)

a_1	1.8399	a_2	0.9450	a_3	2.2152
a_4	2.2227	a_5	0.9779	a_6	1.8883
C_6	2.823[a]	C_8	41.83[a]	C_{10}	871.3[a]

[a] Form Ref. [21]

separations, with our potential being slightly less repulsive than the previous theoretical ones.

In Table 2 the interaction potential has been broken down into repulsive SCF and intra-atom correlation contributions on the one hand (exchange terms), and attractive, intra-atom correlation contributions on the other (dispersion terms). The intra-atom correlation is obtained in a separate CI calculation with double substitutions, which was restricted to the localized (but orthogonal) SCF orbital of He, and the inter-atom correlation is the remaining difference to the total correlation. This analysis follows closely the one first applied to the He–H_2 system [2]. Both components could be fitted very well when only a few parameters were introduced in a slightly generalized Tang–Toennies model [7]:

$$V_{\text{rep}}(R) = (a_1 + a_2 R^{a_3}) \exp(-a_4 R), \tag{1}$$

$$V_{\text{att}}(R) = -a_5 \sum_{n=3}^{9} D_{2n}(a_6 R) C_{2n} R^{-2n} \tag{2}$$

with the incomplete gamma function as damping function:

$$D_m(x) = 1 - \exp(-x) \sum_{k=0}^{m} x^k/k!. \tag{3}$$

The potential is given by the sum of the attractive and repulsive components, $V(R) = V_{\text{rep}}(R) + V_{\text{att}}(R)$. The $a_1, \ldots, a_6$ are the fitting parameters. The first three long-range coefficients C_6, C_8, C_{10}, are taken from the accurate calculation of Ref. [21]. Further coefficients up to C_{18} are obtained from the empirical recursion relation [25]:

$$C_{2n} = (C_{2n-2}/C_{2n-4})^3 C_{2n-6}. \tag{4}$$

Recently recalculated coefficients including C_{12} verified the recursion relation for this coefficient [26]. The scaling factor was initially set to $a_5 = 1$, Eq. (2). With the exponent a_6 as the only fit parameter, all data points of V_{att} were reproduced with an accuracy of 1%. This ansatz contains more C_{2n}-terms than is warranted by the basis set used, but there may be some compensation from the admixture of intra-He correlation introduced by orthogonalizing the atomic orbitals. There is of course some correlation between the damping parameter a_6 and the number of higher-order dispersion coefficients C_{2n}.

The fit of the repulsive part is of similar quality. The weighted fit of the total potential is thus in the 1% range, except of course for the few points near the root of the potential which show fitting errors of the same *absolute* magnitude as the neighboring points. The fit could be further improved by adjusting the scaling parameter a_5 to a value close to unity. The implied "correlation" of the computed long-range coefficients C_{2n} is very small and quite consistent with the limitations of our basis. The resulting best fit parameters and other constants are shown in

Table 4. Well depth ε and position R_m of the minimum of the H–He potential; comparison with previous data

Source	ε (10^{-6} E_h)	R_m (bohr)
Present results	22.56	6.66
Jochemsen et al. [3]	22.03	6.784
Scoles [6]	22.65	6.67
Ray [10]	11.0	7.00
Theodorakopoulos et al. [24]	15.00	6.992
Tonnies et al. [23]	16.9	7.03
Knowles et al. [5]	18.28	6.88
Tang and Yang [1]	18.4	6.87
Das et al. [8]	20.664	6.803
Toennies et al.[a]	25.4	7.03
Ulrich et al. [16]	≈ 27	$\approx 7.$
Davison and Liew [9]	35	$\approx 7.$
Miller and Schaefer[b]	119	$\approx 7.$

[a] Also from Ref. [23]; was deemphasized because of inconsistency with D–He scattering data

[b] J Chem Phys 53:1421 (1970)

Table 3. The quality of the fit of V_{att} with only one adjustable parameter underlines the basic soundness of the Tang–Toennies model for the damped dispersion part of the potential.

The simple exponential repulsion is not quite sufficient for quantitative accuracy at the inner branch, though. The main limitation for a predictive power of the model appears to lie in the ad hoc scaling of the (exponential) SCF potential to account for second order exchange effects. In the present case a scaling of 15% was derived as the geometric mean of the scalings for He_2 and H_2 ($^3\Sigma_u$) and may indeed by overestimated because in He–H one electron is not subject to all exchange effects.

From the analytical model we determine the well depth and position of the minimum to be $\varepsilon = 22.56\ \mu E_h$ and $R_{min} = 6.66$ bohr. The well parameters of various previous potential models are compared in Table 4; these have in the past differed widely.

3 Hyperfine frequency shift

Pressure-induced frequency shifts are conveniently given as relative shifts:

$$\Delta a(R)/a_\infty = (a(R) - a_\infty)/a_\infty, \tag{5}$$

where $a_\infty \approx 1.420405726$ GHz $= a(R)$ for $R \to \infty$ is the familiar hyperfine frequency splitting of the non-interacting H atom [27]. The function, Eq. (5), increases linearly with the helium density (at not too high densities) and is invariant under isotope substitution.

Adrian [28] pointed out that exchange effects cause *positive* frequency shifts which decrease exponentially with separation R. *Negative* frequency shifts, on the other hand, arise from dispersion interactions which may be expanded at long range in terms of inverse powers of separation, $-\sum_{n\geq 3} K_{2n} R^{-2n}$ [28]. Thus, the

Table 5. Relative hyperfine frequency shifts, $\Delta a(R)/a_\infty$, multiplied by 10^6

R	SCF	Intra	Total	D-fit
2.0	− 40951.46	− 10500.06	− 51451.52	− 125.56
2.3	14294.55	− 10490.32	3804.23	217.97
2.5	36069.06	− 8972.86	27096.20	59.08
2.8	40678.48	− 7262.69	33415.79	− 2.72
3.0	37457.71	− 5809.94	31647.77	4.28
3.5	24769.28	− 3703.08	21066.20	− 13.99
4.0	13939.32	− 2400.67	11538.65	− 19.66
4.5	7177.73	− 1557.41	5620.32	− 13.44
5.0	3484.33	− 1001.10	2483.23	− 4.70
5.5	1619.53	− 637.34	982.19	0.93
6.0	729.23	− 404.16	325.08	1.62
6.5	316.04	− 252.22	63.81	0.57
6.8	206.77	− 201.02	5.75	0.13
7.0	134.46	− 160.72	− 26.25	− 0.17
7.5	55.54	− 103.83	− 48.29	− 0.31
8.0	21.56	− 68.06	− 46.50	0.02
9.0	2.04	− 31.27	− 29.22	0.38
10.0	− 0.26	− 15.62	− 15.87	− 0.03
11.0	− 0.61	− 8.37	− 8.97	0.13
12.0	− 0.32	− 4.76	− 5.08	− 0.03
15.0	0.00	− 1.25	− 1.25	− 0.01

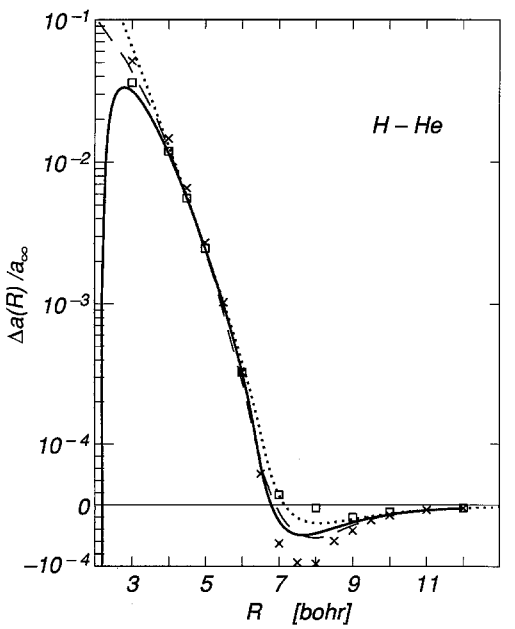

Fig. 2. The hyperfine frequency shifts of H–He: present results (*heavy, solid line*); Jochemsen and Berlinsky's ad hoc model (*dashed*) [3]; Tang and Yang's model (*dotted*) [1]; Ray's results (□) [10]; Davison and Liew's results (×) [9]

hyperfine frequency shift $\Delta a(R)$ mirrors the interatomic potential. For that reason, it is plausible [1] to attempt again an analytical representation similar to Eqs. (1, 2):

$$\Delta a(R)/a_\infty = (c_1 + c_2 R^{c_3}) \exp(-c_4 R) - c_5 \sum_{n=3}^{9} K_{2n} D_{2n}(c_6 R) R^{-2n}, \qquad (6)$$

Table 6. Fit parameters of Eq. (5); for the relative hyperfine shift, $\Delta a(R)/a_\infty$, $K_{12}, \ldots, K_{18}$ from an equation like (4); in atomic units

c_1	−14.530	c_2	1.15320	c_3	3.33048
c_4	2.22110	c_5	0.98313	c_6	1.53633
K_6	13.26[a]	K_8	269.0[a]	K_{10}	7221[a]

[a] From Ref. [29]

where the $c_1, \ldots, c_6$ are fitting parameters. Long-range coefficients K_{2n} with $n = 3, 4$ and 5 have been calculated by Rao et al. [29] and by Greenwood and Tang [30]. The K_6 and K_8 are in agreement but the K_{10} differ by a factor of ≈ 2.5. Our results support clearly the larger K_{10} value of Ref. [29].

Our calculations are based on a spin-unrestricted treatment at both levels, SCF as well as CI, making use of an unrestricted version of our self-consistent electron pair technique [31], combined with the coupled-electron pair approximation (CEPA-1) [32]. Our results are documented in Table 5 and displayed in Fig. 2, together with previous data. Two molecular calculations exist, a generalized valence bond (GVB) treatment by Davison and Liew [9] (crosses, Fig. 2) and an MCSCF calculation by Ray et al. [10] (squares, Fig. 2), which differ significantly in the well region but agree fairly well at shorter range, where the unrestricted Hartree–Fock (UHF) shifts should provide a reasonable approximation. Neither effort accounts for the observed temperature dependence of the shifts. A simple average of the two, used by Jochemsen and Berlinsky [33] (dashed, Fig. 2), agrees with the available measurements reasonably well. At temperatures around 300 K, the model function of Tang and Yang [1] (dotted, Fig. 2) agrees with experiment when used with Tang and Yang's potential, but if fails to reproduce the data at low temperature and the observed isotope shifts.

Our calculated spin density changes are seen to differ from all previous ones but are closest to Jochemsen and Berlinsky's ad hoc average [33]. For distances below $3a_0$ the spin density shows a dramatic turn-around and a change of sign at about $2a_0$. This indicates that the He K-shell starts to extend to the proton and shields it from the unpaired electron, pointing to the formation of a Li type structure. Even so, the analytical fit, Eq. (6), is again very satisfying as seen from the last column of Table 5. The fit parameters of this analytical representation are given in Table 6. The dispersion coefficients $K_{12}, \ldots, K_{18}$ are obtained from a recursion relation like Eq. (4).

Comparison with measurements. In order to compare these results with experiment, we have calculated the statistical average of the shift:

$$\left\langle \frac{\Delta a(R)}{a_\infty} \right\rangle_T = 4\pi\varrho \int_0^\infty \frac{\Delta a(R)}{a_\infty} g(R; T) R^2 \, dR, \tag{7}$$

using our potential and hyperfine frequency shift models, Eqs. (1, 2, 6). The average is a function of temperature T. In Eq. (7), ϱ designates the number density of He and $g(R; T)$ is the H–He pair distribution function. In the low-density limit the pair distribution function is given by [34, 35]:

$$g(R; T) = \lambda_0^3 \int_0^\infty \sum_l \frac{2l+1}{4\pi} \exp(-E/kT) \frac{1}{R^2} |\psi(R; E, l)|^2 \, dE, \tag{8}$$

Table 7. Thermally averaged hyperfine pressure shifts, computational results

T[K]	Classical	Quantum	T[K]	Classical	Quantum
0.5		− 8.06	30.	14.67	16.75
0.5		− 4.57[a]	40.	23.95	25.15
0.7		− 8.20	50.	32.61	33.82
1.0	1391.40	− 8.49	100	70.20	71.19
1.15		− 8.53	150	102.0	102.8
2.0	3.26	− 8.41	200	130.1	130.9
3.0	− 14.63	− 7.92	250	155.7	156.4
4.0	− 15.23	− 7.14	300	179.3	180.1
5.0	− 14.08	− 6.16	350	201.3	202.1
10.0	− 7.15	− 1.36	400	222.0	222.0
12.5		1.13	600	295.5	
16.0	− 1.04	4.59	800	356.9	
20.0	4.52	8.42	1000	410.4	

[a] Value for ^{3}He instead of ^{4}He

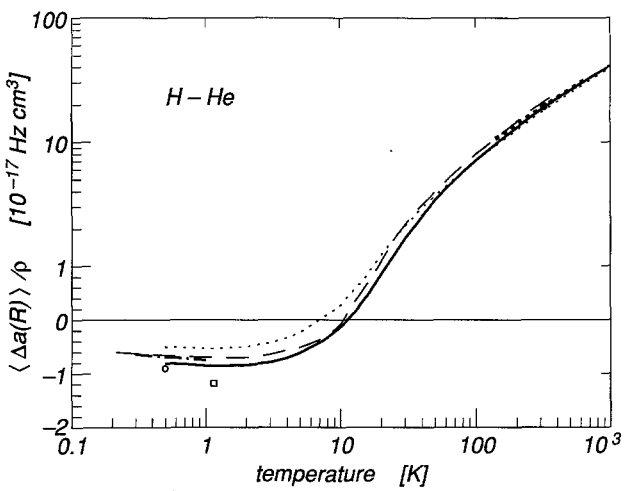

Fig. 3. The pressure-induced hyperfine frequency shifts, normalized by the helium density; present calculation (*solid heavy line*); Jochemsen et al.'s ad hoc model (*dashed*) [33]; Tang and Yang's model (*dotted*) [1]; Pipkin and Lambert's measurement (*big dot*) [12]; Wright et al.'s measurements (*heavy dotted line*) [13]; Hardy et al.'s data (*open square*) [14]; Morrow et al.'s H–^{3}He measurement (*open circle*) (see Ref. [3])

where ψ is the energy-normalized, radial wavefunction of relative motion for translational energy E and angular momentum l; $\lambda_0^2 = 2\pi\hbar^2/mkT$ is the square of the thermal de Broglie wavelength; m is the reduced mass; and k is Boltzmann's constant. At temperatures $T > 40$ K, the semi-classical form of the pair distribution form may be used,

$$g(R;T) = \exp(-V(R)/kT)\left\{1 - \frac{\hbar^2}{12m(kT)^2}\left(V'' + \frac{2}{R}V' - \frac{1}{2kT}(V')^2\right) + \mathcal{O}(\hbar^4)\right\}. \tag{9}$$

The exponential represents the classical expression of the pair distribution function and the term in braces $\{\cdots\}$ is known as the Wigner–Kirkwood quantum correction factor of that classical expression. The computer programs used for the calculations of expressions like Eq. (7) have been described elsewhere [36]. The results are given in Table 7 and Fig. 3.

If the measurement suggests a dependence of the hyperfine frequency shifts on the helium density which is not exactly linear, a virial expansion of the pair distribution function becomes necessary, i.e. an expansion in terms of powers of the H and He densities [34, 37]. At low temperatures the third virial coefficient was found to be of substantial magnitude in other, similar systems.

We note that the surprisingly close agreement between classical and quantum calculations down to about 15 K reported in Ref. [1] may be related to the fact that in that work potential and frequency shift are nearly identical functions of R. Such close agreement down to rather low temperatures cannot be expected in general.

Figure 3 compares our results (heavy, solid lines) with the measurements of the hyperfine frequency shift coefficient $\langle \Delta a \rangle / \varrho$ at various temperatures T. Anderson et al. [11] have obtained a pressure shift of 3.7×10^{-9} torr^{-1} $\pm$ 20% at 50°C, that is $(17.6 \pm 3.5) \times 10^{-17}$ Hz cm^3, in the units employed in Fig. 3. Pipkin and Lambert [12] (solid square in the figure) measured $(22.9 \pm 0.5) \times 10^{-17}$ Hz cm^3 at 45°C.

Wright et al. [13] obtained a relative pressure shift coefficient of $(4.19 \pm 0.2) \times 10^{-9}$ torr^{-1} at 50°C, at a helium pressure of 94.4 torr, when deuterium was substituted for hydrogen (D–He pairs). A nearly linear temperature dependence was observed for temperatures from about -133 to $+365$°C, with relative pressure shifts of 2.55×10^{-9} torr^{-1} at the lower end and 7.09×10^{-9} torr^{-1} at the upper. In order to include these in Fig. 3, we multiply the observed relative shifts by the hyperfine splitting of H instead of D. (The hyperfine frequency splitting of D is 327, 384, 349 Hz [27].)

Hardy et al. [4, 14] provided the point at $T \approx 1.15$ K (open square) and Jochemsen et al. [3] report a measurement by Morrow et al. of H interacting with the rare isotope ^{3}He at temperatures near 0.5 K (open circle). At such low temperatures, the pair distribution function depends strongly on the reduced mass of the pair – in contrast to the region where classical relationships hold. For 0.5 K we have calculated a relative shift of 4.566 for ^{3}He (full circle) as compared to the 8.055 for ^{4}He. While agreement is very satisfactory at temperatures above 10 K, there remains a distinct discrepancy for the measurements around 1 K.

4 Infrared absorption

Dissimilar pairs of interacting atoms absorb light in the far infrared region of the spectrum (collision-induced absorption) [38, 39]. Translational absorption is essentially a molecular process. The absorption proceeds via interaction-induced dipole moments arising from dispersion and electron exchange [40], the same mechanisms that cause intermolecular attraction at long range and repulsion at near range. A recent monograph attempts to summarize our knowledge of interaction-induced dipoles and absorption in the infrared [17].

Table 8. Dipole moment of H–He pairs, in 10^{-6} a.u.; positive values relate to a polarity according to H^-He^+

R	SCF	Intra	Inter	Total	Bsse	D-fit
2.00	396803.49	8356.25	− 9549.03	395610.71	− 5.30	− 120.82
2.25	291343.24	5871.75	− 4415.60	292799.39	− 5.26	− 5.29
2.50	215637.12	4503.83	− 3202.25	216938.70	− 4.49	48.37
2.75	160174.44	3620.69	− 3362.09	160433.04	− 3.62	93.83
3.00	118990.20	2960.51	− 3740.18	118210.53	− 3.03	78.49
3.50	65011.99	1972.67	− 3886.96	63097.70	− 2.64	− 27.21
4.00	34663.78	1266.85	− 3275.94	32654.69	− 2.25	− 59.57
4.50	17928.39	772.95	− 2429.58	16271.76	− 1.70	− 29.71
5.00	8986.89	449.81	− 1663.13	7773.57	− 1.22	− 1.65
5.50	4376.93	248.89	− 1080.54	3545.28	− 0.73	7.41
6.00	2077.50	132.04	− 678.66	1530.88	− 0.45	5.95
6.50	964.28	67.43	− 417.68	614.03	− 0.40	2.56
6.75	651.62	47.97	− 326.12	373.47	− 0.39	1.22
7.00	438.17	33.85	− 254.40	217.62	− 0.30	0.59
7.50	196.47	16.08	− 154.76	57.79	− 0.32	− 0.48
7.50	196.29	15.98	− 154.70	57.57	− 0.18	− 0.26
8.00	86.39	7.42	− 94.75	− 0.94	− 0.12	− 0.05
9.00	15.92	1.48	− 37.08	− 19.68	− 0.07	0.38
10.00	2.72	0.28	− 15.70	− 12.70	− 0.09	0.24
11.00	0.38	0.06	− 7.31	− 6.87	− 0.09	0.10
12.00	0.07	0.01	− 3.71	− 3.63	− 0.08	− 0.03
13.00	0.01	0.00	− 2.03	− 2.02	− 0.04	− 0.03
14.00	0.00	0.00	− 1.18	− 1.18	− 0.02	− 0.02
15.00	0.00	0.00	− 0.72	− 0.72	− 0.02	− 0.01

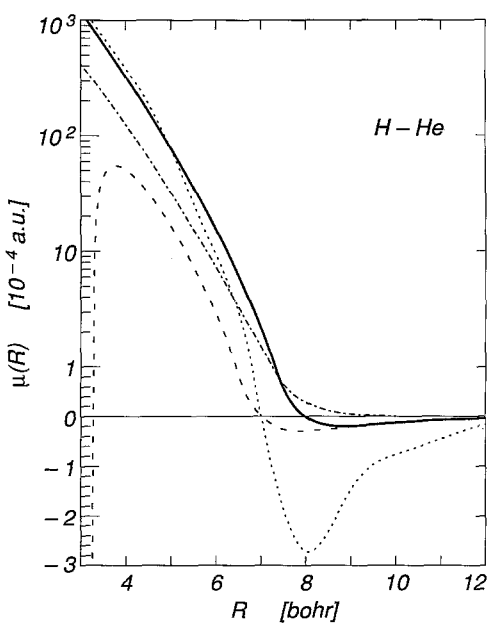

Fig. 4. Interaction-induced dipole moment as function of separation R; present results (*heavy solid curve*). For comparison, the SCF + D_7 model of Brown and associates is shown (*dashes*) [44, 45]; Ulrich, Ford and Browne's data (*dotted*) [16]; and the pure exchange dipole by Lacey and Byers Brown (*dash-dot*) [44]

Table 9. Fit parameters of the induced dipole moment, Eq. (6), in atomic units. All D_n values are zero except those specified here

d_1	6.3645	d_2	0.7144	d_3	2.5210
d_4	1.55045	d_5	0.03354	d_6	1.41000
D_7	122[a]	D_{13}	4.03E7[b]		

[a] From Ref. [45, 46]
[b] Not really a dispersion term

Theoretical attempts to compute induced dipole moment functions of binary complexes have been reviewed elsewhere [15]. Induced dipole moments represent rather small distortions of the electronic charge distributions in response to intermolecular interactions, but as is well known for interaction potentials, the importance of exchange effects limits the applicability of perturbation theory and requires a CI treatment which properly accounts for the coupling between exchange and dispersion effects.

4.1 Induced dipole

The induced dipole moment thus obtained is given in Table 8 as a function of separation. As before, the total dipole moment is given as the sum of exchange contributions from SCF and intra-atom correlation, and dispersion contributions due to inter-atom electron correlation. As for the potential, these terms are seen to be of opposite sign. The superposition error is seen to be quite small. The present computational procedures have been seen in a number of cases to provide dependable, very accurate induced dipole data [15, 41–43]. Figure 4 illustrates the near exponential fall-off of dipole strength μ with separation at near range (solid, heavy curve; down to values of 10^{-5} a.u., a logarithmic scale is employed). We notice a change of sign at separations slightly smaller than 8 bohr, a minimum near 9.2 bohr and a slow rise to 0 at greater separations.

The dipole moment may be represented by an analytical function like:

$$\mu(R) = (d_1 + d_2 R^{d_3}) \exp(-d_4 R - d_5 R^2) - \sum_{n=3}^{6} D_{2n+1}(d_6 R) D_{2n+1} R^{-2n-1}. \tag{10}$$

The parameters $d_1, \ldots, d_6$ of the fit are given in Table 9.

Previous work. The H–He pair, the simplest realistic diatom composed of unlike atoms, has played a special role in previous attempts of computing interaction-induced dipoles [40, 44, 45]. Interest in this system is, however, not solely theoretical. It has been pointed out that absorption of infrared radiation by H–He pairs is likely to be an important source of opacity in the atmospheres of the late stars [16] where neutral atomic hydrogen and helium exist in significant amounts and ionization is negligible.

In the first calculation of the H–He dipole moment, Buckingham clearly demonstrated the exchange and dispersion origins of the induced moments [40]. In a more quantitative attempt, Lacey and Byers Brown derived an exchange dipole from undistorted HF atom wavefunctions but obtained only about 1/3 of the present dipole strength [44]. Whisnant and Byers Brown computed the leading

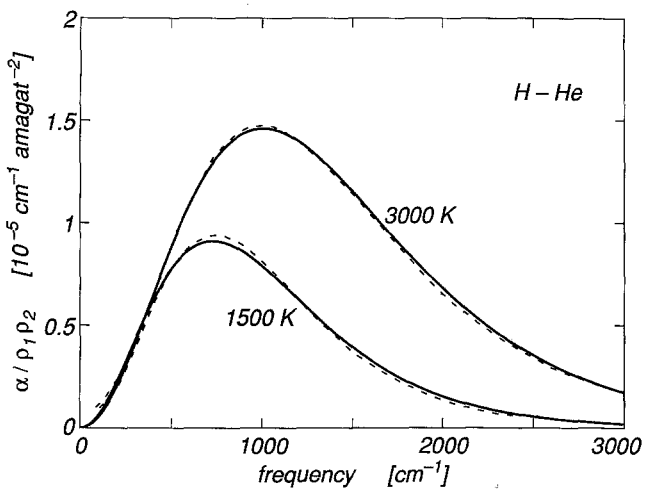

Fig. 5. The absorption coefficient, normalized by the hydrogen and helium densities, as function of frequency, at two temperatures. The *dashed lines* represent Ulrich, Ford and Browne's computational results [16]

dispersion dipole coefficient and obtained $D_7 = 122$ a.u. for H–He, with a polarity as H^+He^- [45]. Recent work by Bohr and Hunt confirms this value [46]. Our (dispersion) dipole moment is consistent with this D_7 value for the largest distances but it increases more strongly for shorter separations R and is not compatible with the usual inverse-power expansion. We attribute this to a rather far-reaching effect due to overlap of diffuse dispersion functions. In the analytic representation, this is taken care of by the D_{13} coefficient which must not be mistaken for a true dispersion term. The 28-term CI wavefunction of Ulrich et al. [16] should have been capable of producing a realistic dipole function. There is indeed fair agreement at shorter distances ($\pm$ 15%), but at large distances the results deviate totally, probably because of uncontrolled basis superposition errors (dotted curve of Fig. 4). Also shown in Fig. 4 are Lacey's pure exchange dipole [44] (dot-dash) and the so-called SCF + D_7 model (dashes), combining Lacey's exchange dipole with the lowest-order dispersion term, $-D_7/R^7$ [45].

Summarizing, it may be said that the previous theoretical data describing the H–He dipole moment are rather inconsistent, in particular for the larger internuclear separations. No experimental data exist for this system for comparison. We may note that our previous induced dipole calculations for several other systems are in excellent agreement with the existing measurements [41–43, 47, 48]. In view of the simple structure of the system under consideration the present data are believed to be of an even better precision.

4.2 Absorption spectra

Computing the absorption spectra from the dipole and potential data is straightforward [15–17]. The absorption coefficient α is given by:

$$\alpha(\omega; T) = \frac{4\pi^2}{3\hbar c} \varrho(\mathrm{H})\, \varrho(\mathrm{He})\, \omega \left[1 - \exp\left(\frac{-\hbar\omega}{kT}\right)\right] Vg(\omega; T). \tag{11}$$

In this expression, ω designates angular frequency; and $Vg(\omega; T)$ is the spectral density which we compute from a quantum formalism described elsewhere [17]. The precision of the line shape calculations has been checked with the help of the three lowest-order sum rules as usual [17]. The spectral moments determined by integration of the spectral profiles agreed with the quantum-mechanical sum rules at the 1% level.

Figure 5 shows the computed absorption for two temperatures of astrophysical interest. At these high temperatures our results are in reasonable agreement with those of Ref. [16], the differences of potential and induced dipole surfaces (which are most striking at low energies) notwithstanding.

5 Conclusion

We have reported an accurate potential surface, hyperfine frequency shifts and induced dipole surface computed from first principles for H–He pairs, paying special attention to the delicate balances of exchange and dispersion effects in the broad vicinity of the potential minimum. The data obtained permit in general accurate comparisons with the existing measurements.

Acknowledgements. We thank N. G. Hardee for computing the spectra shown in Fig. 5 as solid lines. The work was supported by the *Sonderforschungsbereich 91* of the Deutsche Forschungsgemeinschaft. For the work at the University of Texas, the support of the R.A. Welsh Foundation, grant F-988, is acknowledged.

References

1. Tang KT, Yang XD (1990) Phys Rev A42:311
2. Meyer W, Hariharan PC, Kutzelnigg W (1980) J Chem Phys 73:1880
3. Jochemsen R, Berlinsky AJ, Hardy WN (1984) Can J Phys 62:751
4. Hardy WN, Morrow M, Jochemsen R, Statt BW, Kubik PR, Marsolais RM, Berlinsky AJ, Landesman A (1980) Phys Rev Lett 45:453
5. Knowles DB, Murrell JN, Braga JP (1984) Chem Phys Lett 110:40
6. Scoles G; Appendix of Ref. [3]
7. Tang KT, Toennies JP (1984) J Chem Phys 80:3726. See also references therein.
8. Das G, Wagner AF, Wahl AC (1978) J Chem Phys 68:4917
9. Davison WD, Liew YC (1972) J Phys B5:309
10. Ray S (1975) Phys Rev A12:2031
11. Anderson LW, Pipkin FM, Baird JC Jr (1960) Phys Rev 120:1279. Erratum (1961) ibid 122:1962
12. Pipkin FM, Lambert RH (1962) Phys Rev 127:787
13. Wright JJ, Balling LC, Lambert RH (1970) Phys Rev A1:1018
14. Hardy WN, Morrow M, Jochemsen R, Berlinsky AJ (1982) Physica 109 & 110 B:1964
15. Meyer W (1985) ab initio calculations of collision-induced dipole moments. in: Birhbaum G (ed) Phenomena induced by intermolec interactions. Plenum Press, NY, p 29
16. Ulrich BT, Ford L, Browne JC (1972) J Chem Phys 57:2906
17. Frommhold L (1993) Collision-induced absorption in gases. Cambridge Univ Press, NY
18. Werner HJ, Reinsch EA (1982) J Chem Phys 76:3144; Meyer W (1978) in: Schaefer HF III (ed) Methods of electronic structure theory. Vol IIIa, Plenum, NY, p 413
19. Huzinaga S (1964) J Chem Phys 42:1293
20. Boys SF, Bernardi F (1970) Mol Phys 42:73
21. Koide A, Meath WJ, Allnatt AR (1982) J Phys Chem 86:122
22. Gengenbach G, Hahn C, Toennies JP (1973) Phys Rev A1:98

23. Toennies JP, Welz W, Wolf G (1976) Chem Phys Lett 44:5
24. Theodorakopoulos G, Farantos SC, Buenker RJ, Peyerimhoff SD (1984) J Phys B: At Mol Phys 17:1453
25. Tang KT, Toennies JP (1978) J Chem Phys 68:5001
26. Spelsberg D, Meyer W, to be published
27. Anderson LW, Pipkin FM, Baird JC Jr (1960) Phys Rev 120:1279
28. Adrian FJ (1960) J Chem Phys 32:972
29. Rao BK, Ikenberry D, Das TP (1970) Phys Rev A2:1411
30. Greenwood WG, Tang KT (1987) J Chem Phys 86:3539
31. Flesch J (1982) Thesis, Univ of Kaiserslautern; Meyer W (1976) J Chem Phys 64:2901
32. Meyer W (1973) J Chem Phys 58:1017
33. Jochemsen R, Berlinsky AJ (1982) Can J Phys 60:252
34. de Boer J (1949) Physica 15:680
35. Hirschfelder JO, Curtiss CF, Bird RB (1964) Molecular theory of gases and liquids. Wiley, NY
36. Moraldi M, Borysow A, Frommhold L (1984) Chem Phys 86:339
37. Moraldi M, Frommhold L (1989) Phys Rev A40:6260
38. Kiss ZJ, Welsh HL (1959) Phys Rev Lett 2:166
39. Poll JD, van Kranendonk J (1961) Can J Phys 39:189
40. Buckingham AD (1959) L'absorption des ondes micrométriques induite pur la pression dans des gaz non-polaries. In: Colloques Internationaux du C.N.R.S., vol 77, p 57, Paris
41. Meyer W, Frommhold L (1986) Phys Rev A33:3807
42. Meyer W, Frommhold L (1986) Phys Rev A 34:2771
43. Meyer W, Frommhold L (1986) Phys Rev A 34:2936
44. Lacey AJ, Byers Brown W (1974) Molec Phys 27:1013
45. Whisnant DM, Byers Brown W (1973) Molec Phys 26:1105
46. Bohr JE, Hunt KLC (1987) J Chem Phys 86:5441
47. Frommhold L, Meyer W (1987) Phys Rev A 35:632. Erratum: (1990) Phys Rev A41:534
48. Meyer W, Frommhold L, Birnbaum G (1989) Phys Rev A 39:2434